
CASE REPORT

Giant Cell Tumour of the Axial Skeleton: Report of Four Cases

NY Pan^{1*}, CY Law^{1△}, WK Tsang^{2#}, KL Lee³, KC Wong¹, KF Tam⁴

¹Department of Radiology, Kwong Wah Hospital, Yaumatei, Hong Kong; ²Department of Diagnostic Radiology and Nuclear Medicine, Tuen Mun Hospital, Tuen Mun, Hong Kong; ³Department of Imaging and Interventional Radiology, Prince of Wales Hospital, Shatin, Hong Kong; and ⁴Department of Radiology, North District Hospital, Sheung Shui, Hong Kong

* Currently at Department of Radiology, Princess Margaret Hospital, Hong Kong

△ Currently at Department of Radiology, Caritas Medical Centre, Hong Kong

Currently at Department of Radiology and Imaging, Queen Elizabeth Hospital, Hong Kong

ABSTRACT

Giant cell tumours are locally aggressive benign bone lesions with typical imaging features. Giant cell tumours can affect virtually any part of the body, but tend to be situated in the appendicular skeleton, with the axial skeleton being an uncommon site of occurrence. This report is of four patients with axial giant cell tumour, two involving the thoracic spine, one involving the sacrum, and one involving the temporal bone, with corresponding clinical presentations and imaging findings.

Key Words: Giant cell tumors; Sacrum; Spine; Temporal bone

中文摘要

中軸骨骼之巨細胞瘤：四宗病例報告

潘寧遠、羅俊逸、曾慧勤、李嘉樂、黃國俊、譚國輝

巨細胞瘤是一種具局部侵略性的良性骨骼病變，其影像特徵典型。巨細胞瘤幾乎可以發生於全身任何部位，但好發於附肢骨骼，而中軸骨骼不是常見發病部位。本文報告四宗中軸骨骼的巨細胞瘤病例，闡述相應臨牀表現及影像特徵。四個病例之中，兩宗病灶位於胸椎，一宗位於骶骨，一宗位於顳骨。

INTRODUCTION

Giant cell tumours (GCTs) of the bone are locally aggressive lesions that primarily affect the epiphyses of the long bones. Lesions of the axial skeleton that affect the thoracic spine, sacrum, and temporal bone are rare occurrences. This article describes these uncommon

presentations of GCTs in four patients, with their corresponding clinical and imaging features.

CASE REPORTS

All four patients were referred to our institutions between 2006 and 2012. All patients had preoperative

Correspondence: Dr Nin-yuan Pan, Department of Radiology, Princess Margaret Hospital, Kwai Chung, Hong Kong. Tel: (852) 6461 0074; Fax: (852) 2990 2697; Email: blueorca1981@gmail.com

Submitted: 1 Dec 2011; Accepted: 29 Jul 2013.

imaging with computed tomography (CT) and magnetic resonance imaging (MRI). Histological diagnosis of GCT was obtained before or at surgery in all four cases. Relevant clinical data were retrieved via the electronic patient record database.

Case 1

In March 2010, a 40-year-old previously healthy woman presented to Kwong Wah Hospital with acute lower back pain precipitated by a fall. On physical examination, there was no lower limb neurology or sphincter dysfunction.

Radiographs of the thoracolumbar junction of a T11 vertebral body showed a compression fracture

with an underlying osteolytic lesion. Plain CT of the thoracolumbar spine showed a bubbly, expansile lytic lesion that had almost entirely infiltrated the T11 vertebra, involving both its anterior and posterior elements (Figure 1). The lesion contained a burst fracture, which generated a retropulsed fragment causing focal spinal stenosis. The lesion did not cross the intervertebral discs into the adjacent vertebrae, nor did it breach the costovertebral and costotransverse joints to invade the ribs. Apart from the pathological fractures, the cortical bone was diffusely thinned, but largely intact, without sclerotic changes. The lesion possessed no substantial extraosseous soft-tissue component. Internal trabeculations were present, although no matrix calcification, ossification, or ground-

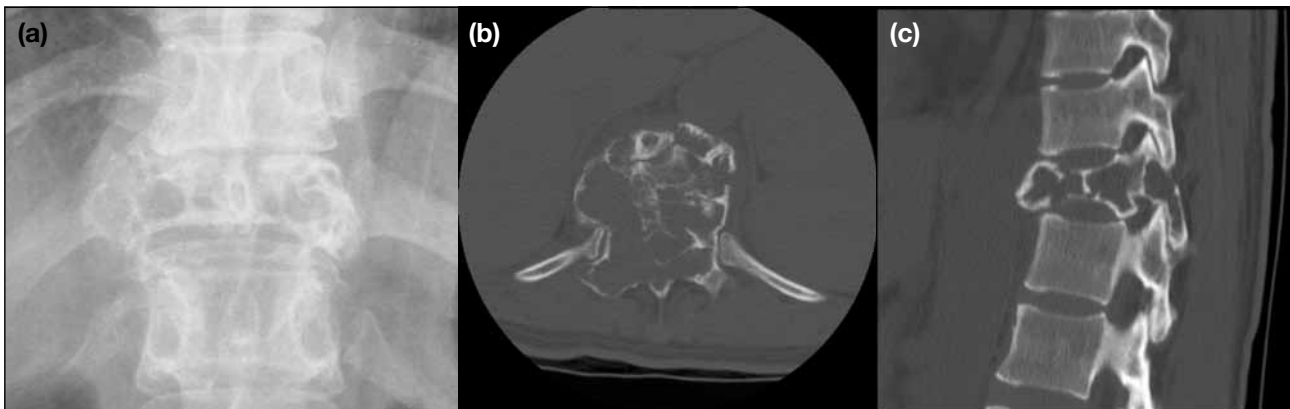


Figure 1. Imaging of patient 1. (a) Anterior-posterior chest radiograph at presentation shows a collapsed T11 vertebral body. The outline of the pedicles is still preserved and visibly expanded. (b) Axial and (c) sagittal multislice computed tomography images through the T11 vertebra show an expansile lytic lesion involving both the anterior and posterior elements with complicating collapsed fracture. Internal trabeculations are present without visible matrix mineralisation. There is no associated paraspinal soft-tissue component or extension into adjacent vertebrae.

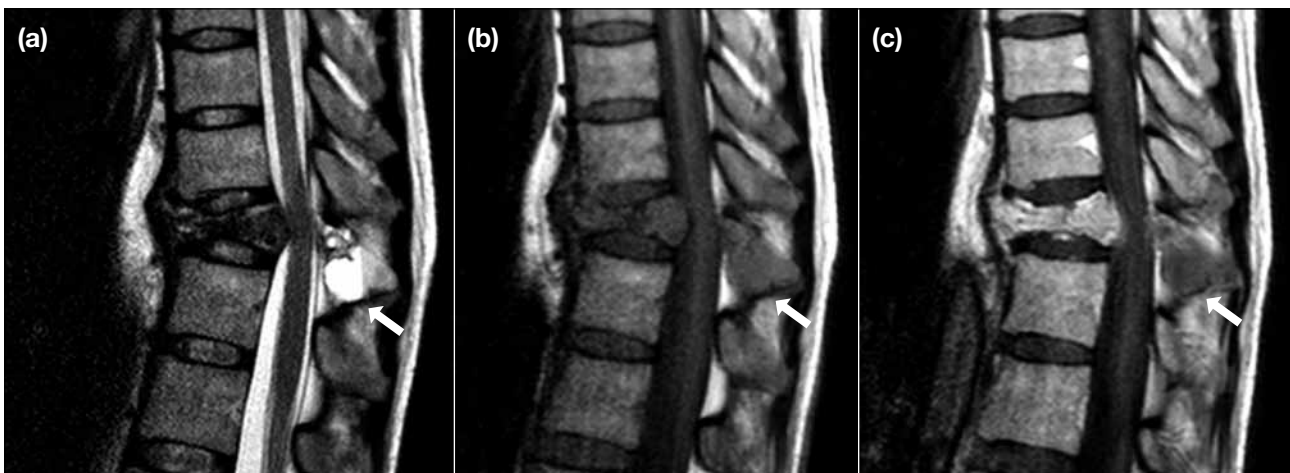


Figure 2. Magnetic resonance imaging of patient 1 shows (a) an expansile mass in the T11 vertebra of mixed signal on T2-weighting and (b) predominantly low signal on T1-weighting (c) with significant enhancement after gadolinium contrast injection (arrows). Note the presence of bony retropulsion causing compression of the spinal cord and an associated secondary aneurysmal bone cyst with fluid-fluid levels.

glass opacity was visible.

Subsequent MRI with gadolinium contrast (Figure 2) showed an expansile lesion within the collapsed T11 vertebra, with low T1-weighted signal and heterogeneous mixed signal intensity, but predominantly hypointense T2-weighted signal intensity in the vertebral body. More cystic changes were seen in the posterior element suggesting secondary change of an aneurysmal bone cyst. Closed biopsy of the T11 vertebra under local anaesthesia confirmed GCT of the bone.

One month later, laminectomy from T11 to L1 was performed with excision and curettage of the tumour, followed by posterior spinal fusion and application of fixation plates. A durotomy and patch repair was also required at the T11 level due to dural adhesion by the tumour found during surgery. The final pathological diagnosis was GCT.

The patient remained well postoperatively. The most

recent follow-up CT scan, performed 2 years after the operation, showed no evidence of recurrence.

Case 2

In July 2006, a 46-year-old woman presented to Princess Margaret Hospital with throbbing pain over the right temporal region for several months, with a gradual increase in severity. The pain was aggravated by jaw motion and relieved with over-the-counter analgesics. No associated hearing loss or tinnitus was experienced. She had good past health other than diabetes mellitus, which was managed with oral anti-hyperglycaemic agents.

On physical examination there was an immobile hard tender subcutaneous 2-cm swelling in the right temporal region, without involvement of the overlying skin. There was mild limitation to the degree of jaw opening.

Plain and contrast-enhanced axial CT showed a roundish 3.0 x 3.7-cm expansile lytic lesion centred on the right squamous temporal bone (Figure 3). The lesion

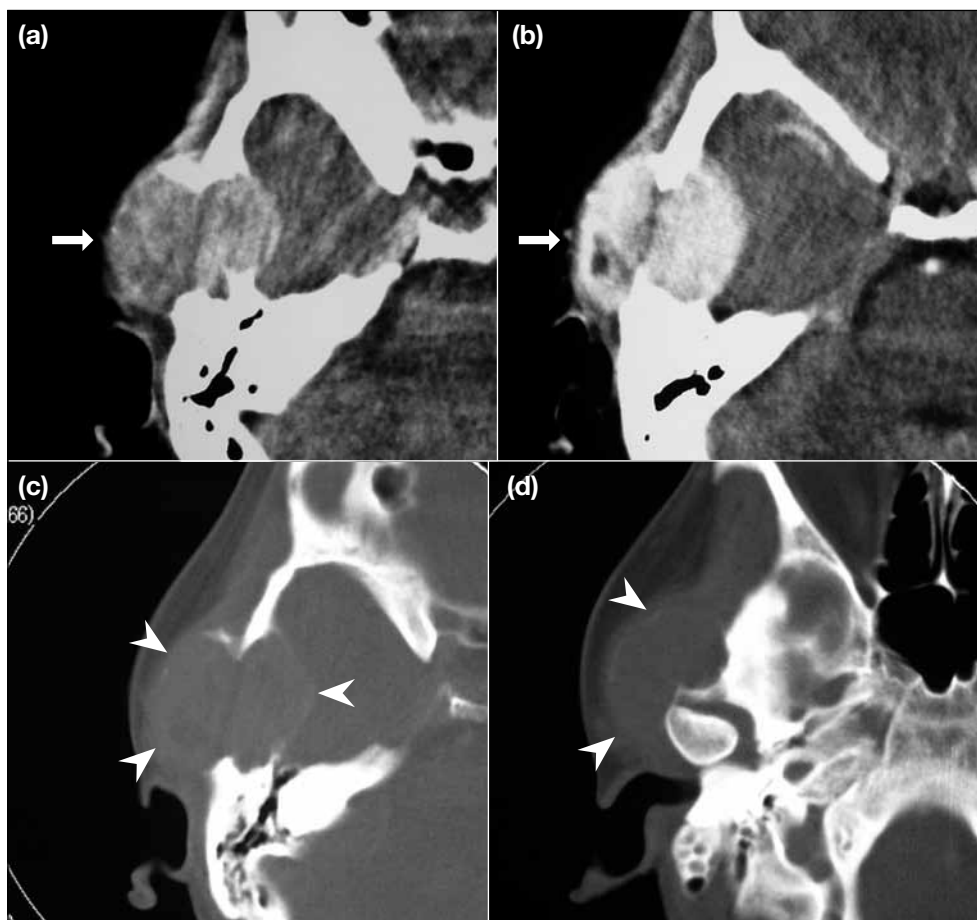


Figure 3. Axial computed tomography images through the right temporal bone of patient 2 show (a) a roundish soft-tissue mass centred on and destroying the squamous portion of the temporal bone (arrow), extending laterally into the pre-auricular subcutaneous soft tissue and medially into the middle cranial fossa. (b) Significant enhancement is seen after contrast injection (arrow). (c and d). Bone window shows an expansile lytic mass (arrowheads), which is abutting, but not involving the temporomandibular joint. No matrix calcification is visible.

had completely eroded the adjacent inner and outer skull tables, and possessed a large extraosseous component expanding laterally into the pre-auricular subcutaneous tissue and medially into the middle cranial fossa. There was also anterior extension with destruction of the posterior zygomatic arch. Inferiorly, the lesion extended to the subarticular region of the mandibular fossa, but did not show intra-articular extension. There was no matrix calcification or ossification visible. The lesion exhibited heterogeneous hyperenhancement after contrast injection.

MRI showed a mass that was predominantly hypointense on T1-weighted and T2-weighted images, with heterogeneous contrast enhancement. Inferiorly, the lesion abutted the temporomandibular joint without invading it (Figure 4), concurring with the CT findings.

Pathological analysis of a fine-needle aspiration sample was inconclusive, and was summarised as a giant cell-rich lesion, probably benign. Differential diagnoses include hyperparathyroid bone disease, giant cell

reparative granuloma, solid variant of aneurysmal bone cyst, GCT, and other giant cell-containing lesions.

Subsequent whole-body bone scintigraphy with ^{99m}technetium-labelled methylene diphosphonate showed the lesion to be the only site of involvement with no other focal radionuclide uptake.

Craniectomy was performed, with frozen section findings compatible with GCT. Intra-operatively, the tumour was found to have infiltrated the dura mater and was adherent to, but separable from, the temporomandibular joint capsule. The tumour was extirpated along with the adherent dura. Specimen histology confirmed the diagnosis of GCT with clear resection margins.

Postoperatively the patient completed a course of adjuvant radiotherapy (50 Gy in 25 Fr). Since then she has had annual CT follow-up, and has demonstrated no local recurrence on her most recent CT performed 6 years postoperatively.

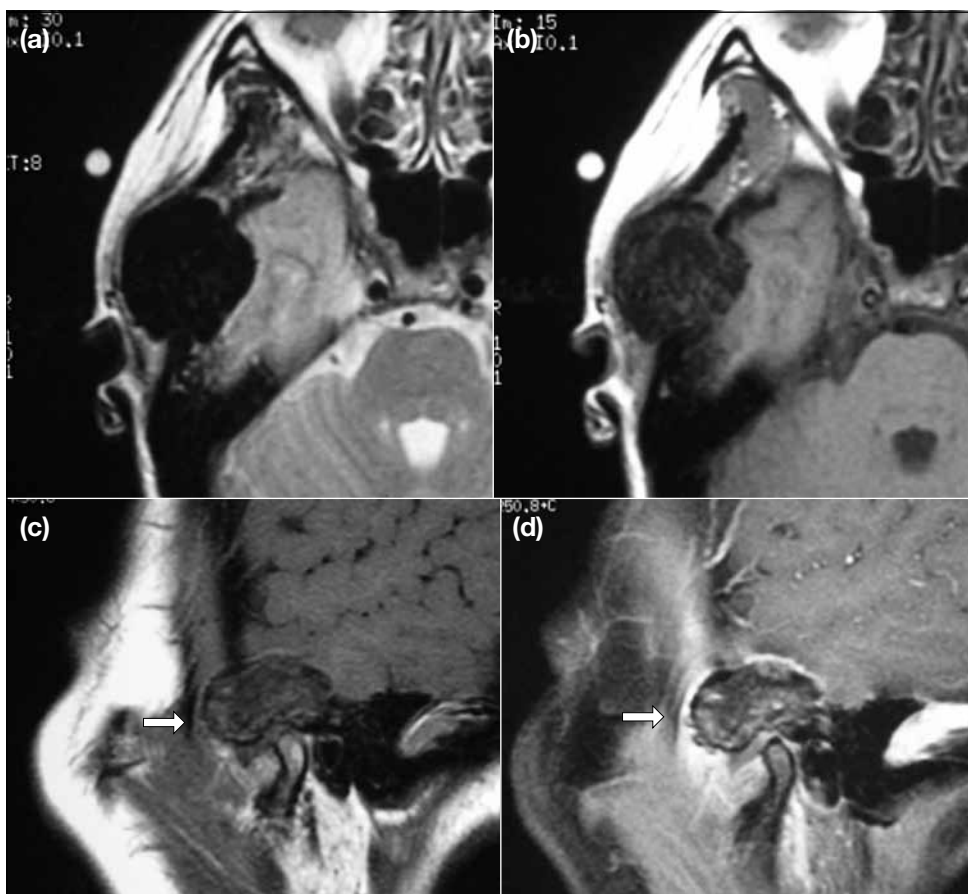


Figure 4. Magnetic resonance images of patient 2. Transverse (a) T1- and (b) T2-weighted images show a roundish mass centred on the right petrous temporal bone with predominantly low signal intensity. Sagittal (c) pre- and (d) post-gadolinium T1-weighted images show enhancement after contrast injection. The subarticular location of the lesion can be appreciated on the sagittal images (arrows). The hypointense rim present on both the T1- and T2-weighted sequences is probably due to haemosiderin deposition.

Case 3

In June 2007, a 54-year-old man with unremarkable past health presented to Prince of Wales Hospital with bilateral sacral pain for several months, which was more severe on the right side. The pain appeared insidiously and had steadily progressed, being present both nocturnally and at rest. There was no radiation or referral of pain to the lower limbs. The patient also experienced faecal incontinence and urinary retention. No constitutional symptoms were present.

On physical examination, no mass was palpable over the lower back, but localised deep tenderness was evident on applying pressure to the right sacral region. No deficit was demonstrated on neurological examination

of the lower limbs. Anal sphincter tone was found to be reduced.

Radiographs showed an ill-defined expansile lytic lesion in the right sacral region (Figure 5a). CT showed a large osteolytic mass involving most of the sacrum with infiltration into the spinal canal, right greater sciatic notch, and right sacroiliac joint (Figure 5b to 5d). The mass had heterogeneous enhancement and was not calcified. MRI showed intermediate signal intensity on T1- and T2-weighted images and heterogeneous post-gadolinium enhancement (Figure 6). Pathological analysis of CT-guided core biopsy confirmed the diagnosis of GCT.

The patient underwent preoperative embolisation of the

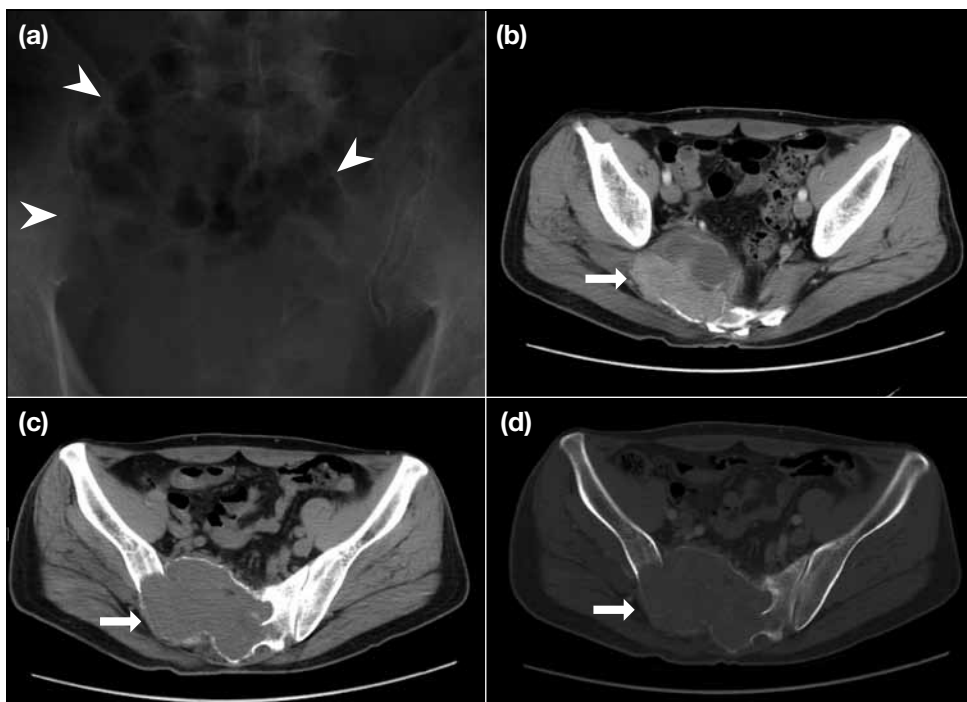


Figure 5. Images of patient 3 at presentation. (a) Radiograph shows ill-defined osteolysis involving mainly the right sacrum with extension to the lower half of the right sacroiliac joint (arrowheads). (b to d) Subsequent axial post-contrast computed tomography images show an expansile, heterogeneously enhancing non-calcified mass destroying the central and right sacrum, invading the sacral spinal canal, sacral foramina, and right greater sciatic notch (arrows).

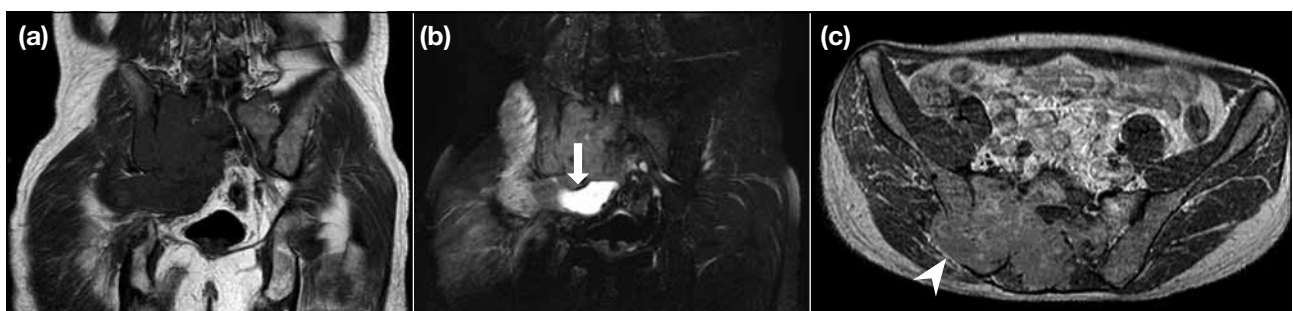


Figure 6. Magnetic resonance images of patient 3. (a) T1-weighted and (b) fat-suppressed T2-weighted images show the central and right sacral mass to be predominantly solid with a small cystic component (arrow) at its inferior aspect. The rest of the mass is of low T1-weighted and intermediate T2-weighted signal intensity. (c) Post-contrast T1-weighted image shows lesional enhancement (arrowhead).

right internal iliac artery, followed by radical resection and curettage of the tumour. He also received multiple perioperative infusions of zoledronic acid (4 mg intravenous infusions, with two infusions given within 1 month preoperatively and monthly infusions given for 3 months postoperatively), a bisphosphonate which was devised to improve local control.

Postoperatively the patient was neurologically stable. Urinary and bowel symptoms were managed with intermittent catheterization and pelvic floor exercises, respectively, and the patient returned to work while taking analgesics for residual back pain. Serial follow-up imaging showed residual right sacral tumour, which remained stable in size while the patient received scheduled infusions of zoledronic acid.

One year after the last infusion of zoledronic acid, and 4 years after the initial presentation, the patient presented acutely with deep venous thrombosis of the right lower limb. The patient was otherwise stable without deterioration in pain or neurological symptoms, and was still able to work. CT and MRI showed tumour progression, involving the left sacral wing and posterior elements of the S1 vertebra (Figure 7). Pre-sacral extension of the tumour accounted for compression of

the right common iliac vein leading to thrombosis.

The patient did not wish to undergo a second operation and preferred a trial of denosumab (given as 120 mg intravenous injections monthly for 6 months). Latest reassessment imaging (MRI) of the pelvis for treatment response performed in February 2014 showed progression in the extent of the sacral tumour.

Case 4

In March 2012, a previously healthy 28-year-old woman presented to Tuen Mun Hospital with sudden bilateral lower limb weakness, inability to walk, and acute urinary retention for 1 day. She had previously experienced mid- and lower back pain for several months, which was dull and progressive without radiation or referral. She received local analgesic injections from her family doctor with short durations of improvement. She had no constitutional symptoms.

On physical examination, there was significant reduction in power in the right lower limb and mild weakness in the left lower limb, while sensory testing was essentially intact. Sphincter tone was normal on rectal examination.

Radiographs of the thoracic spine showed complete

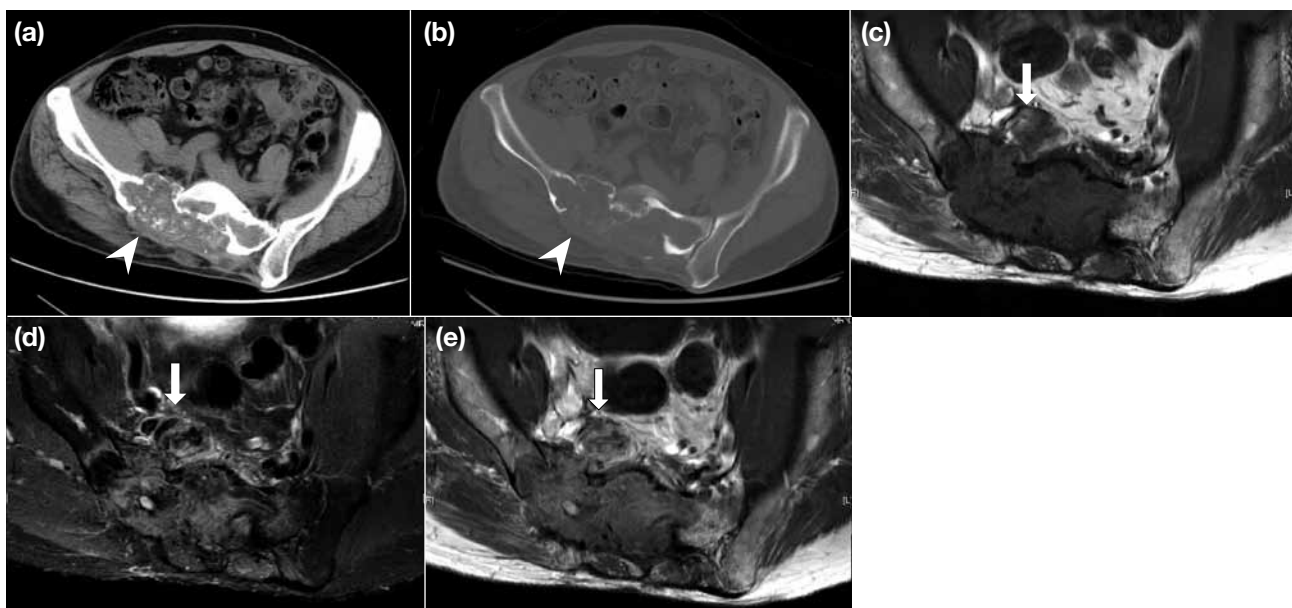


Figure 7. Images of patient 3 four years after presentation. (a and b) Computed tomography images show progression of the sacral mass that has spread into the left sacrum. Amorphous calcifications are present within the mass (arrowheads). (c) T1-weighted, (d) T2-weighted, and (e) T1-weighted post-gadolinium magnetic resonance images show pre-sacral extension of tumour (arrows) compressing on the right common iliac vein, which leads to venous thrombosis. Internal low signal foci correspond to calcification on correlation with the computed tomography images.

collapse of the T10 vertebral body, resulting in vertebra plana (Figure 8). Adjacent disc spaces were preserved and there was a left paraspinal soft-tissue mass from the T9 to T11 levels.

CT showed a markedly flattened anterior two-thirds of the T10 vertebral body, while the posterior third bulged posteriorly into the spinal canal (Figure 9).

MRI showed epidural soft-tissue components which compressed the thecal sac and spinal cord bilaterally (Figure 10). Bilateral paraspinal soft-tissue components were also present, with the left-sided component showing deep extension medial to the parietal pleura to reach the posterior mediastinum. The solid soft-tissue components were of intermediate T1-weighted signal intensity and low T2-weighted signal intensity, while

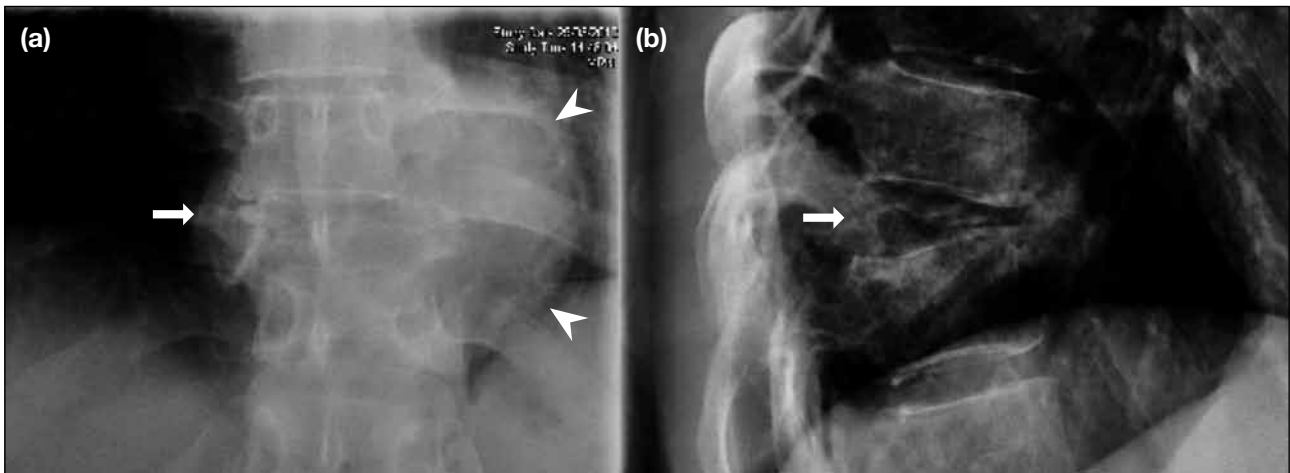


Figure 8. (a) Frontal and (b) lateral radiographs of the lower thoracic spine of patient 4 at presentation show complete collapse of the T10 vertebral body, with relatively well-preserved adjacent disc spaces (arrows). Neither of the T10 pedicles are visible on frontal view. A left paraspinal soft-tissue mass is visible along T9 to T11 levels (arrowheads).



Figure 9. (a) Coronal and (b) axial computed tomography scans of the lower thoracic spine of patient 4 show a lytic expansile mass in the T10 vertebra, with internal matrix calcifications. The lesion had infiltrated the bilateral pedicles and the left transverse process. There is a large left paraspinal component that spreads anteriorly along the medial aspect of the pleural space reaching the posterior mediastinum (arrowheads).

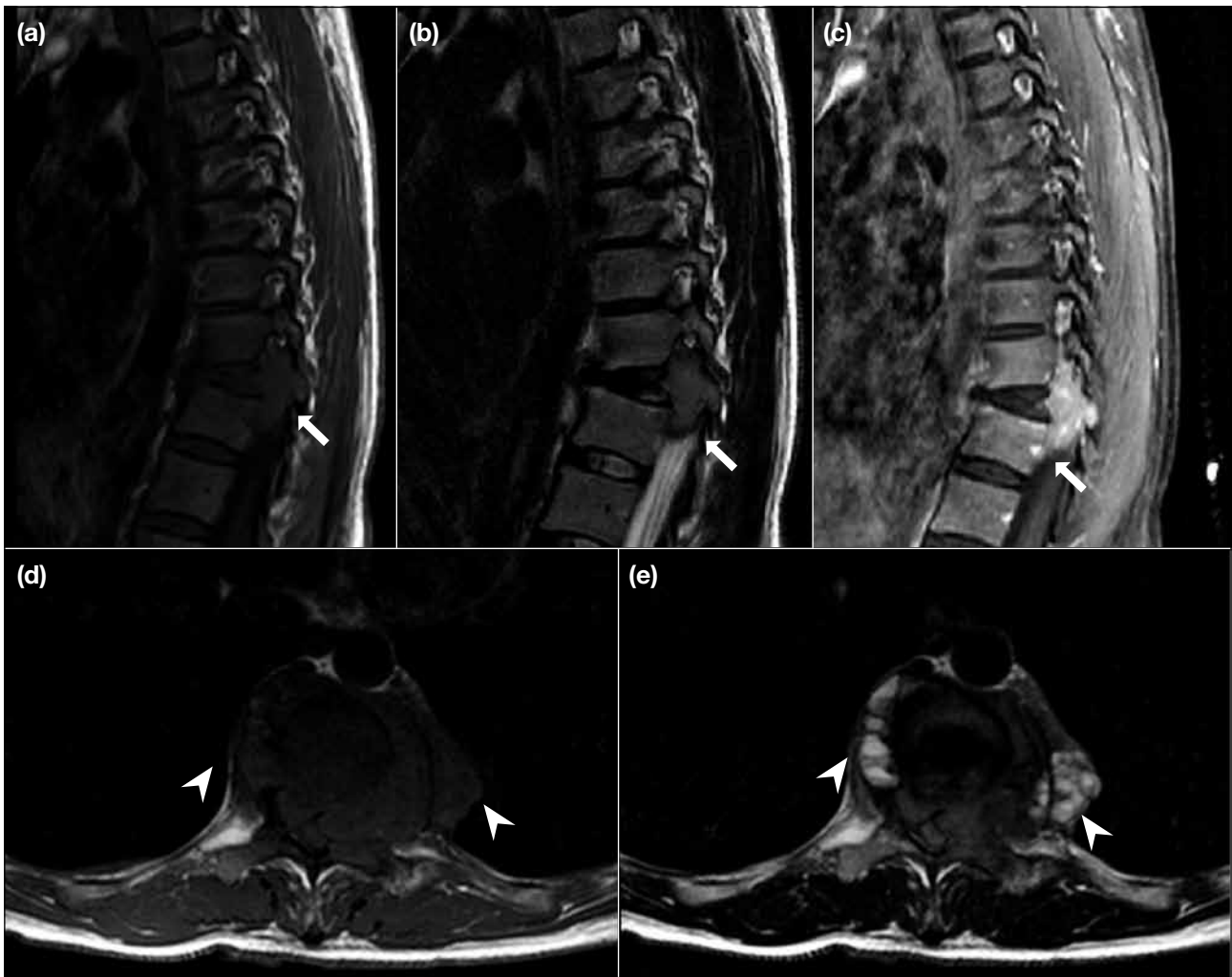


Figure 10. Magnetic resonance images of patient 4. (a) T1-weighted, (b) T2-weighted, and (c) post-contrast T1-weighted images show the mass to be of low T1- and T2-weighted signal intensity with post-contrast enhancement (arrows). Axial (d) T1-weighted and (e) T2-weighted images show bilateral paraspinal cystic components with fluid-fluid levels, consistent with co-existent secondary aneurysmal bone cysts (arrowheads).

paraspinal cystic components with fluid-fluid levels were compatible with associated aneurysmal bone cysts.

The patient underwent urgent surgical decompression with tumour resection and posterior spinal fusion from the T8 to L1 levels. A separate surgery involving left thoracotomy and anterior spinal fusion was required to treat the deep left paraspinal component. Pathology on the resected specimens from both operations confirmed GCT.

Postoperatively, the patient fully regained her lower limb power and sphincter functions. She also received radiation therapy and multiple zoledronic acid infusions (4 mg intravenously every 4 weeks for 6 months). Latest

follow-up MRI in July 2013 showed no local recurrence of tumour.

DISCUSSION

GCTs are locally aggressive primary bone neoplasms, which characteristically involve the epiphyses of long bones. GCTs affecting other parts of the skeleton are rare, but this entity must be considered in the differential diagnosis of any expansile osteolytic lesion. Dahlin¹ found an incidence rate for GCT of 4.2% of 6221 bone tumours.

GCTs have a predilection for women, mainly presenting in the second to fourth decades of life with a peak in the third decade of life.² GCTs are prevalent in China

and India, where they account for up to 20% of all primary bone tumours.^{2,3} Most GCTs arise in the end of long bones, particularly around the knee joint. Only a minority (3%-5%) occur in the spine and craniofacial regions.⁴⁻⁷ The vast majority (99%) of GCTs are solitary.^{1,2} Three of these four patients were women, in keeping with demographic observations.

Spinal GCTs are rare, accounting for about 2% to 3% of all GCTs.⁴ The most commonly affected site is the sacrum, followed by the thoracic, cervical, and lumbar segments in decreasing order of frequency.⁸ GCTs have a predilection for the vertebral body with frequent involvement of posterior elements,⁹ as in these patients. Lesions limited to the posterior elements are uncommon and account for only 21%.⁹ Intervertebral disc involvement and invasion of adjacent vertebrae are possible, but did not occur in these patients. Secondary aneurysmal bone cysts, representing erythrocyte 'lakes' probably formed during episodes of haemorrhage,¹⁰ are a known associated finding in the mobile spine. Spinal GCTs commonly present as pain (often with a radicular distribution), weakness, and sensory deficits.⁸

Craniofacial GCTs are even rarer than spinal GCTs and form only 1% to 2% of all GCTs. Craniofacial GCTs preferentially affect the sphenoid, ethmoid, and temporal bones as these bones develop partially or entirely from endochondral ossification.^{5,11,12} Paget's disease also predisposes to craniofacial GCTs.¹³ Patients with craniofacial GCTs are typically older men with an established history of Paget's disease, and polyostotic involvement is common. Otagia, headache, hearing loss, and cranial nerve palsies are common presenting symptoms for temporal bone GCTs.^{6,13}

CT is ideal for depicting expansile bony remodelling, cortical thinning, presence of periosteal reaction, and pathological fractures.² CT also demonstrates a lack of sclerotic margins, absence of matrix mineralisation, and subarticular relationship with the adjacent joint, which are important for narrowing the differential diagnosis.² Calcification is uncommon in GCTs and suggests an alternative diagnosis of chordoma, chondrosarcoma, craniopharyngioma, or meningioma.² Giant-cell reparative granuloma, another cause of an expansile lytic lesion, has a similar radiographic appearance, but more often occurs in the mandible, maxilla, hands, and feet.²

Radiological diagnosis of GCT relies on its subarticular

location, as up to 99% reach within 1 cm of subarticular bone.² All four patients described in this series had GCTs that involved subarticular bone, with the thoracic spinal lesions being related to the uncovertebral and costovertebral joints, the sacral lesion related to the right sacroiliac joint, and the temporal bone lesion related to the temporomandibular joint. The precise origin of GCTs remains a topic of debate, although recent arguments appear to favour an origin from the metaphyseal side of the physal plate. This is supported by the observation that, in the rare case of involvement in a skeletally immature patient, the lesion often extends towards the diaphysis rather than the epiphysis, with the open physal plate acting as a barrier.²

MRI is ideal for determining soft-tissue extension and for lesional characterisation. GCTs are usually low-to-intermediate in T1- and T2-weighted signal, and are contrast-enhancing.² The relative T2-weighted low signal intensity is probably due to the relatively high collagen and haemosiderin content.¹⁰ In patient 1, the mixed T2-weighted signal intensity in the lesion was most likely due to oedema from a recent pathological fracture. The low T2-weighted signal intensity is useful for differentiating GCTs from other entities such as a large solitary subchondral cyst, intraosseous ganglion, Brodie abscess, or clear chondrosarcoma which demonstrate high T2-weighted signal intensity.¹⁴

Differential diagnosis of an expansile lytic lesion involving anterior spinal elements includes metastasis, lymphoma, chordoma, myeloma, plasmacytoma, and eosinophilic granuloma.⁹ MRI is also useful for narrowing the differential list, as most of the other lesions have high T2-weighted signal intensity.¹⁵⁻¹⁷ Chordomas tend to be situated in the sacrum, and are calcified in about 90% of cases.⁹ GCTs are usually non-calcified. In patient 3, the matrix calcifications appearing in the second set of CT and MRI images were probably post-treatment effects, as GCTs are known to exhibit sclerotic changes following bisphosphonate treatment.^{18,19}

Cranial GCTs lack distinctively diagnostic radiological characteristics.¹⁴ Metastases and plasmacytomas are common in the skull and radiographically indistinguishable from GCTs. Eosinophilic granulomas are a consideration in younger patients, although multifocal involvement is usually present.¹⁶ Osteosarcomas, chondrosarcomas, and chordomas are characterised by matrix mineralisation and anatomical

predilections such as the petro-occipital fissure for chondrosarcomas and the clivus for chordomas.¹⁵ MRI is a useful aid to distinguish GCTs from the other lesions, which generally have high T2-weighted signal intensity.¹⁴⁻¹⁷

Surgical excision with negative margins remains the treatment of choice for cranial GCTs.¹³ Disease control after complete resection is 85% to 90% successful in the peripheral skeleton. However, spinal lesions, particularly sacral ones, have a poorer prognosis because the lesions are larger and difficult to excise completely,¹⁰ as in patient 3. Radiation therapy is controversial,¹³ but is probably an acceptable means of limiting the risk of recurrence, particularly when disease is locally extensive or if complete removal is difficult. Patients 2 and 4 underwent postoperative adjuvant radiotherapy.

Denosumab is a monoclonal antibody that targets the receptor activator of nuclear factor κ -B ligand and stops the osteoclastic activity in GCTs.²⁰ Dramatic treatment responses have been reported, with at least 90% tumour necrosis in some phase 2 trials,²⁰ raising the drug's prospects as a stand-alone treatment for poor surgical candidates or for patients in whom the tumour is in a difficult location to treat surgically.

Some studies have also evaluated the role of zoledronic acid, a bisphosphonate, in the treatment of GCTs through inhibition of osteoclastic function and inducing intralésional cellular apoptosis.^{18,19} Significant reductions in local recurrence rates have been achieved with peri-operative intravenous zoledronate infusions.¹⁸

In summary, GCTs of the axial skeleton are rare. Imaging diagnosis is often challenging, but the combined use of CT and MRI can be useful for characterisation and extent evaluation. Diagnosis ultimately relies on histological analysis for most patients. The prognosis for axial GCTs is poorer than for appendicular lesions due to difficulties in complete surgical removal, although adjunctive radiotherapy and medical therapy may prove useful in the future.

REFERENCES

1. Dahlin DC. Bone tumours. 2nd ed. Springfield, Illinois: Charles C Thomas; 1970.
2. Murphey MD, Nomikos GC, Flemming DJ, Gannon FH, Temple HT, Kransdorf MJ. From the archives of AFIP. Imaging of giant cell tumor and giant cell reparative granuloma of bone: radiologic-pathologic correlation. *Radiographics*. 2001;21:1283-309. [cross ref](#)
3. Sung HW, Kuo DP, Shu WP, Chai YB, Liu CC, Li SM. Giant-cell tumor of bone: analysis of two hundred and eight cases in Chinese patients. *J Bone Joint Surg Am*. 1982;64:755-61.
4. Shankman S, Greenspan A, Klein MJ, Lewis MM. Giant cell tumor of the ischium. A report of two cases and review of the literature. *Skeletal Radiol*. 1988;17:46-51. [cross ref](#)
5. Lee HJ, Lum C. Giant-cell tumor of the skull base. *Neuroradiology*. 1999;41:305-7. [cross ref](#)
6. Rock JP, Mahmood A, Cramer HB. Giant cell tumor of the skull base. *Am J Otol*. 1994;15:268-72.
7. Bertoni F, Unni KK, Beabout JW, Ebersold MJ. Giant cell tumor of the skull. *Cancer*. 1992;70:1124-32. [cross ref](#)
8. Sanjay BK, Sim FH, Unni KK, McLeod RA, Klassen RA. Giant-cell tumours of the spine. *J Bone Joint Surg Br*. 1993;75:148-54.
9. Rodallec MH, Feydy A, Larousserie F, Anract P, Campagna R, Babinet A, et al. Diagnostic imaging of solitary tumors of the spine: what to do and say. *Radiographics*. 2008;28:1019-41. [cross ref](#)
10. Kwon JW, Chung HW, Cho EY, Hong SH, Choi SH, Yoon YC, et al. MRI findings of giant cell tumors of the spine. *AJR Am J Roentgenol*. 2007;189:246-50. [cross ref](#)
11. Leonard J, Gökden M, Kyriakos M, Derdeyn CP, Rich KM. Malignant giant-cell tumor of the parietal bone: case report and review of the literature. *Neurosurgery*. 2001;48:424-9.
12. Lu ZH, Yao ZW. Giant cell tumour of the posterior cranial fossa: a case report. *Br J Radiol*. 2011;84:e206-9. [cross ref](#)
13. Isaacson B, Berryhill W, Arts HA. Giant-cell tumors of the temporal bone: management strategies. *Skull Base*. 2009;19:291-301. [cross ref](#)
14. Lee JA, Bank WO, Gonzalez-Melendez M, Olan WJ, Tabbara SO. Giant cell tumor of the skull. *Radiographics*. 1998;18:1295-1302. [cross ref](#)
15. Erdem E, Angtuaco EC, Van Hemert R, Park JS, Al-Mefty O. Comprehensive review of intracranial chordoma. *Radiographics*. 2003;23:995-1009. [cross ref](#)
16. Stull MA, Kransdorf MJ, Devaney KO. Langerhans cell histiocytosis of bone. *Radiographics*. 1992;12:801-23. [cross ref](#)
17. Hanrahan CJ, Christensen CR, Crim JR. Current concepts in the evaluation of multiple myeloma with MR imaging and FDG PET/CT. *Radiographics*. 2010;30:127-42. [cross ref](#)
18. Tse LF, Wong KC, Kumta SM, Huang L, Chow TC, Griffith JF. Bisphosphonates reduce local recurrence in extremity giant cell tumor of bone: a case-control study. *Bone*. 2008;42:68-73. [cross ref](#)
19. Arpornchayanon O, Leerapun T. Effectiveness of intravenous bisphosphonate in treatment of giant cell tumor: a case report and review of the literature. *J Med Assoc Thai*. 2008;91:1609-12.
20. Chakarun CJ, Forrester DM, Gottsegen CJ, Patel DB, White EA, Matcuk GR Jr. Giant cell tumor of bone: review, mimics, and new developments in treatment. *Radiographics*. 2013;33:197-211. [cross ref](#)